

# A Light Tolerant Neural Recording IC for Near-Infrared-Powered Free Floating Motes

Jongyup Lim<sup>1</sup>, Jungho Lee<sup>1</sup>, Eunseong Moon<sup>1</sup>, Michael Barrow<sup>1</sup>, Gabriele Atzeni<sup>2</sup>, Joseph Letner<sup>1</sup>, Joseph Costello<sup>1</sup>, Samuel R. Nason<sup>1</sup>, Paras R. Patel<sup>1</sup>, Parag G. Patil<sup>1</sup>, Hun-Seok Kim<sup>1</sup>, Cynthia A. Chestek<sup>1</sup>, Jamie Phillips<sup>1,3</sup>, David Blaauw<sup>1</sup>, Dennis Sylvester<sup>1</sup>, Taekwang Jang<sup>2</sup>  
<sup>1</sup>University of Michigan, MI, <sup>2</sup>ETH Zürich, Switzerland, and <sup>3</sup>University of Delaware, DE. (email: jongyup@umich.edu)

## Abstract

A key challenge for near-infrared (NIR) powered neural recording ICs is to maintain robust operation in the presence of parasitic short circuit current from junction diodes when exposed to light. This is especially so when intentional currents are kept small to reduce power consumption. We present a neural recording IC that is tolerant up to 300  $\mu\text{W}/\text{mm}^2$  light exposure (above tissue limit) and consumes 0.57  $\mu\text{W}$  at 38°C, making it lowest power among standalone motes while incorporating on-chip feature extraction and individual gain control.

## Introduction

Power transmission and communication are the key challenge for ultra-small ( $< 0.5\text{mm}$ ) wireless neural recording motes and, among several approaches (RF, ultra-sound [1,2]), NIR using an integrated PV and LED is unique in its ability to scale linearly to very small sizes ( $< 100\mu\text{m}$ ) [3,4]. Minimum size is critical to achieving dense recording arrays and minimum scarring and requires that radiated light power is maximized while chip power and currents are minimized. This leaves the circuits particularly susceptible to light-induced parasitic currents (Fig. 2). In conventional chips, light is blocked with an encapsulant. However, a partly transparent encapsulation that exposes the PV and LED while blocking light for sensitive circuits is infeasible at sub-mm scales leaving the solution to light tolerant circuit design. To our knowledge, this work is the first attempt to address this challenge.

The proposed IC achieves robust operation past the tissue limit NIR ( $150 \mu\text{W}/\text{mm}^2$ ) while a baseline implementation fails at  $8\mu\text{W}/\text{mm}^2$ . The chip maintains sub- $\mu\text{W}$  power while incorporating advanced functionality, including on chip feature extraction and gain control. The proposed work was tested with neural signals from a Long Evans rat and demonstrated high fidelity monkey finger motion decoding.

The envisioned system architecture is described in [4] and consists of a large number of free-floating motes on top of the brain that use NIR for power delivery, uplink and downlink to a repeater unit outside the dura (Fig.1). Each mote consists of a custom GaAs chip with dual junction PV ( $I_{\text{sc}} > 1.1\mu\text{A}$ ,  $V_{\text{oc}} = 1.6\text{V}$  at  $150\mu\text{W}/\text{mm}^2$  850nm light, measured) and LED sandwiched on top of the CMOS chip with an attached carbon fiber penetrating the brain to obtain neural signals.

## Proposed Circuit

The IC consists of a three-stage-amplifier for neural signal acquisition, signal processing that extracts a neural feature called spiking band power (SBP) [5], a pulse gap modulator (PGM) and LED driver for data uplink, and an optical receiver (ORx) for data downlink followed by clock and data recovery (Fig. 3). A pseudo resistor ( $R_{\text{PSD}}$ ) is frequently use for DC-feedback since its high,  $T\Omega$  resistance [3,4] can achieve the demandingly low high-pass corner and reduces resistor noise. However, its extremely low conductance,  $G_{\text{FB}}$ , also makes it susceptible to junction to substrate and deep n-well to p-well photo generated current ( $I_{\text{SC}_P}$ ) (Fig. 4, left). This low conductance vs.  $I_{\text{SC}_P}$  results in a poor *light robustness ratio* ( $R_{\text{LR}} = G_{\text{FB}} / I_{\text{SC}_P}$ ) and the DC-bias level will drift at  $< 1\mu\text{W}/\text{mm}^2$  (simulation). A series-to-parallel switched capacitor-based resistor [7] was proposed to address the process sensitivity of  $R_{\text{PSD}}$ . However, while it has higher conduction, its high number of switches results in a large total junction area and high  $I_{\text{SC}_P}$  and  $R_{\text{LR}}$  remains poor (Fig. 4, mid). Instead, this work adopts a hybrid approach combining a simple switched capacitor resistor with a  $3\times$  attenuator. It maintains a much larger  $G_{\text{FB}}$  while having a lower  $I_{\text{SC}_P}$  resulting a  $5\cdot 10^4\times$  improvement in  $R_{\text{LR}}$  and achieves light tolerance till  $350\mu\text{W}/\text{mm}^2$  in simulation (Fig. 4, right).

The amplifier achieves 68 dB peak gain, [380, 1060] Hz bandwidth,  $> 67\text{dB}$  of CMRR and PSRR and, IRN of  $6.2\mu\text{V}_{\text{RMS}}$  with  $150\mu\text{W}/\text{mm}^2$  of incident 850nm LED light at 38°C in measurement which is nearly unchanged from that measured without light (Fig. 5, table). The graph in Fig. 5 plots measured gain across light level for a baseline  $R_{\text{PSD}}$  and

proposed structure showing that while the baseline structure fails at  $8\mu\text{W}/\text{mm}^2$ , the proposed structure stays stable till  $300\mu\text{W}/\text{mm}^2$ .

Spiking band power (SBP) is a neural feature used for motor prediction and is defined as average of absolute signal amplitude in 300-1000Hz [5]. The analog SBP extraction in [4] is compact, but relies on tens of pA of on-current to charge an integration capacitor, which is susceptible to  $I_{\text{SC}_P}$ . We instead propose an area-efficient and light tolerant *digital* SBP extraction unit using a flash ADC. It consists of a diode-stack-based  $V_{\text{REF}}$  generator (12nA, simulation), dynamic comparators with staggered clocks, followed by pulse generators. An asynchronous counter accumulates the total number of fired pulses which integrates the absolute amplitude over the pulse width (Fig. 6, 7). By comparing the counter to a threshold, SBP is symbol-interval-encoded (LED\_EN, Fig. 6). LED\_EN then fires the LED with a pulse-gap-modulated (PGM) encoding of the mote ID (Fig. 3). Each LED packet consists of a total 17 pulses where the pulse gap ( $2\cdot T_{\text{CLK}}/3\cdot T_{\text{CLK}}$  for data 0/1) encodes the 10b unique chip ID (from PUF [6]) and 6b gain configuration (Fig. 10). The LED driver consumes 76nW (simulation) at 50Hz LED firing rate.

The ORx allows for data downlink and remote gain control (RGC) (Fig. 9). Two matched 2T-VRs [8] provide DC-bias to the inputs of a hysteretic comparator, AC coupled to  $V_{\text{DD}}$  and GND. Light modulation toggles the comparator which drives clock and data recovery. The 2T-VRs are size for 1.4nA (simulation) to ensure light robustness, eliminating the light sensitive  $R_{\text{PSD}}$  bias in [4].

## Measurements

The proposed IC was fabricated in 180nm CMOS (Fig. 11). In a fully wireless optical setup with an NIR laser for power transfer and downlink and SPAD detector for uplink reception (Fig. 10) the IC with custom PV/LED GaAs chip wirebonded side-by-side was fully functional. The LED\_EN signal was successfully decoded from the measured SPAD output using the 16b match filter, shown in Fig. 10.

*In vivo* measurement using a carbon fiber inserted into the brain of an anesthetized Long Evans rat and wired to the CMOS chip verified the proposed SBP extraction. Compared to SBP measurement with a high-power commercial recording/signal-processing system, the proposed chip shows good accuracy for motor function decoding (Fig. 8). All procedures complied with the University of Michigan's Institutional Animal Care and Use Committee.

Finger movement of a monkey was predicted using a 20-channel-recorded motor cortex signal and the resulting SBP from the IC with both fixed gain and off-chip RGC (based on average LED firing rate, Fig. 12a). A Kalman filter was used for training with the first 100s and predicting the next 24s of the movement. The proposed SBP successfully predicted the movement (Fig. 12b) with only slight accuracy degradation. With RGC, accuracy improves by several percent and LED firing rate remains below 50Hz across all the channels, allowing for increased channel utilization.

Table I compares the IC to state-of-the-art standalone wireless recorders. Only optical units scale below 0.5 mm and only the proposed optical mote can fully function under  $300\mu\text{W}/\text{mm}^2$  of light exposure. It also achieves the lowest power consumption of 0.57 $\mu\text{W}$  at 38°C with 4.1 NEF, pseudo-resistor-less amplifier, on-chip SBP extraction in digital domain, and individual mote downlink for RGC.

## Acknowledgements

We thank NIH (5R21EY029452-02) for support.

## References

- [1] J. Lee, *et al.*, NER, 2019.
- [2] M. Ghanbari, *et al.*, JSSC, Nov. 2019.
- [3] S. Lee, *et al.*, TBioCAS, Oct. 2018.
- [4] J. Lim, *et al.*, ISSCC, 2020.
- [5] S. R. Nason, *et al.*, Nature BME, Jul. 2020.
- [6] K. Yang, *et al.*, ISSCC, 2017.
- [7] N. Verma, *et al.*, JSSC, Mar. 2010.
- [8] M. Seok, *et al.*, JSSC, Oct. 2012.

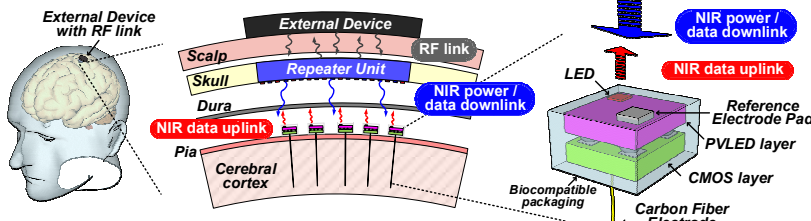


Fig. 1. Conceptual illustration of NIR based wireless neural recording motes

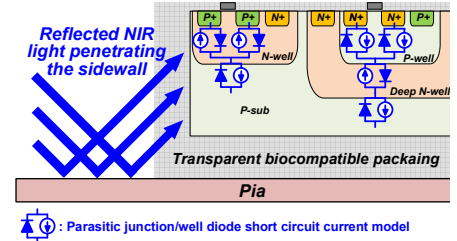


Fig. 2. Cross section of the CMOS layer with parasitic diode short circuit currents

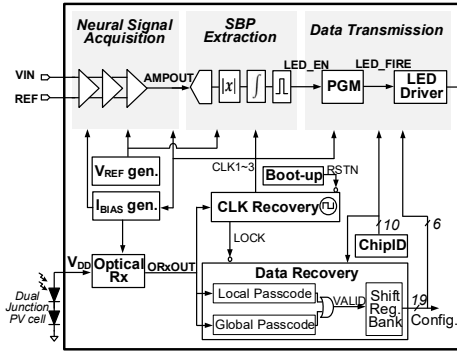


Fig. 3. Top circuit diagram of the CMOS layer

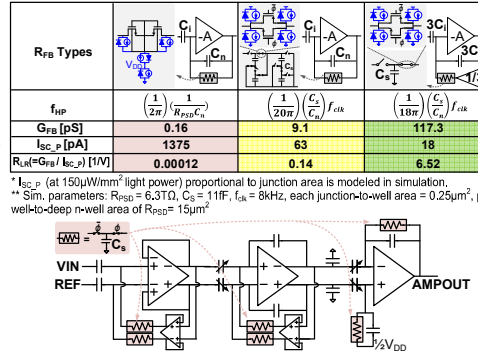


Fig. 4. Simulated light robustness of three different feedback resistors (top) and proposed light tolerant amplifier (bottom)

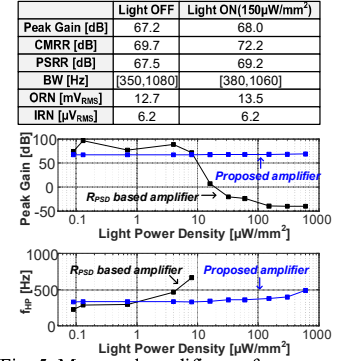


Fig. 5. Measured amplifier performance with 850nm light (IRS4, CMVision)

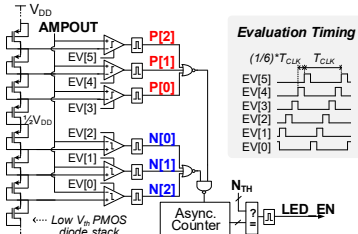


Fig. 6. Flash ADC and pulse-counter-based SBP computing unit

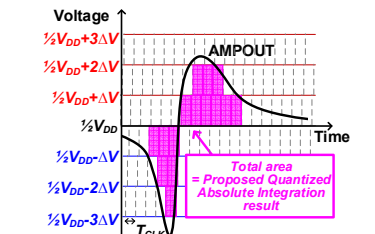


Fig. 7. Quantization of absolute amplitude and width from the SBP computing unit

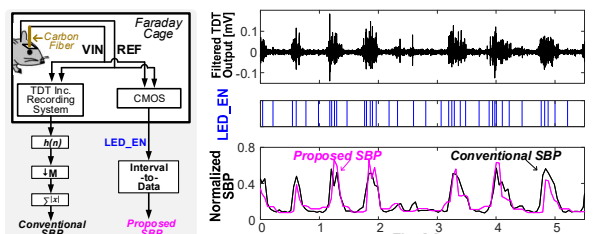


Fig. 8. In vivo measurement setup with RA16PA pre-amp and RX7 Pentusa base station from TDT Inc. (left) and measured waveforms (right)

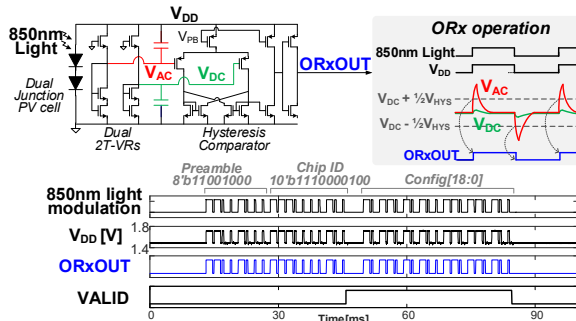


Fig. 9. ORx structure and operation (top), and measured selective programming waveforms from wireless optical setup (bottom)

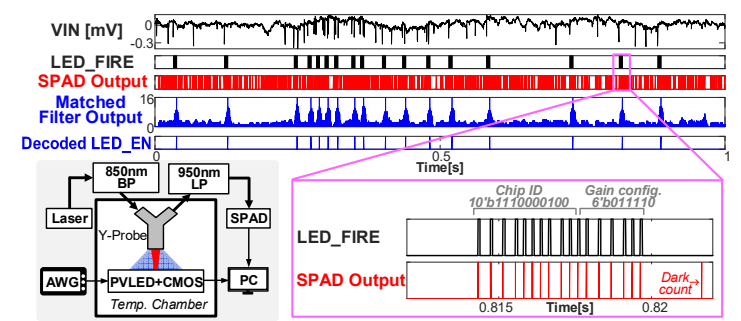


Fig. 10. Measured matched filter decoding result (top), and wireless optical setup with NIR laser (QFLD850200S, Qphotonics) and SPAD (SPDOEMNIR, Aurea) (bottom, left)

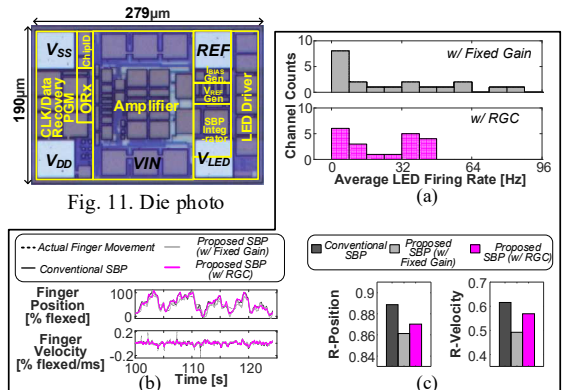


Fig. 11. Die photo

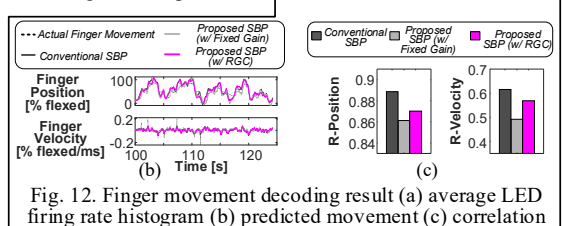


Fig. 12. Finger movement decoding result (a) average LED firing rate histogram (b) predicted movement (c) correlation

Table I. Comparison table

	This work	[4]	[3]	[1]	[2]
Technology [nm]	180	180	180	65	65
Wireless Method	Optical	Optical	Optical	RF	Ultrasonic
Area [mm <sup>2</sup> ] (W [mm] x L [mm])	0.053 (0.19 x 0.28)	0.032 (0.19 x 0.17)	0.014 (0.25 x 0.06)	0.250 (0.50 x 0.50)	0.250 (0.50 x 0.50)
Data Link	UpLink: PGM-SIM DownLink: PWM	Macchester-SIM	PPM	RF	AM
On-chip Feature Extraction	Yes	No	No	No	No
SBP (analog)	Yes	Yes	No	No	No
Chip ID	Yes	Yes	No	Yes	Yes
Clock Recovery	Yes	Yes	No	No	No
Use of Pseudo Resistor	No	Yes	Yes	No	No
Light Tolerant Design (max. light power density)	Yes (300 μW/mm <sup>2</sup> )	No	No	N/A**	N/A**
Supply [V]	1.55	1.5	0.9	0.6	1
Power					
Total [μW]	0.57*	0.74*	1	40	28.8
Amplifier [μW]	0.36*	0.51*	0.5	3.2	4
Target neural signal	AP	AP	LFP, AP	ECOG	LFP, AP
Gain [dB]	67.2*	69.0*	30.0	N/A	24.0
Bandwidth [Hz]	[350, 1080]*	[180, 950]*	10000	500	5000
NEF	4.10*	3.76*	4.31	8.70	5.87

\* Measured at 38°C \*\* Not Applicable